Anatomical Parameterization for Volumetric Meshing of the Liver

Sergio Vera[1 2] Miguel A. González Ballester[1 3 4] Debora Gil[2]

[1]Alma IT Systems, Barcelona, Spain;
[2]Computer Vision Center, Comp. Science Dep., Universitat Autònoma de Barcelona, Spain;
[3]ICREA - Catalan Institution for Research and Advanced Studies, Barcelona, Spain;
[4]Universitat Pompeu Fabra, Barcelona, Spain.

ABSTRACT

A coordinate system describing the interior of organs is a powerful tool for a systematic localization of injured tissue. If the same coordinate values are assigned to specific anatomical landmarks, the coordinate system allows integration of data across different medical image modalities. Harmonic mappings have been used to produce parametric coordinate systems over the surface of anatomical shapes, given their flexibility to set values at specific locations through boundary conditions. However, most of the existing implementations in medical imaging restrict to either anatomical surfaces, or the depth coordinate with boundary conditions is given at sites of limited geometric diversity. In this paper we present a method for anatomical volumetric parameterization that extends current harmonic parameterizations to the interior anatomy using information provided by the volume medial surface. We have applied the methodology to define a common reference system for the liver shape and functional anatomy. This reference system sets a solid base for creating anatomical models of the patient's liver, and allows comparing livers from several patients in a common framework of reference.

Keywords: C oordinate System, Anatomy Modeling, Parameterization.

1. INTRODUCTION

The segmentation based on the liver's vascular system proposed by Couinaud[1] divided that organ into eight segments (territories). This allowed transplantation of whole liver segments from living donors. Recent studies[2] show that transplant success depends greatly on the similarity between the segments of the donor and the receptor. An anatomical coordinate system will put livers from different patients into correspondence without explicitly performing image registration. These coordinates may be obtained through parameterization of the liver anatomy, providing a reference system for comparison of inter-patient data.[3–5]

A parameterization[6,7] of a given n-dimensional topological manifold is defined in the context of differential geometry by one to one local maps between the manifold and a domain of the n-dimensional Euclidean space. Parameterizations generate regular coordinate meshes by taking into account the level curves of the parameterization on the volume. It is important for defining valid coordinate curves from parametric maps that they are smooth (diffeomorphic) functions. Therefore, harmonic functions that solve the Laplacian equation with Dirichlet boundary conditions have been proposed to assess the problem. Dirichlet boundary condition allow setting specific coordinate values at some anatomical sites.[8] The coordinates fixed on such sites propagate over the whole domain and, thus, their variation uniquely determines the parametric map.

Harmonic maps have been used in medical imaging for defining surface mappings on spherical organs, such as the brain,[5,9] but aside from,[10] the potential of harmonic Partial Differential Equations (PDE) for generate coordinates in the whole 3D volume of complex anatomies has been hardly explored. In the definition of coordinate systems adapted to the anatomy geometry a radial or depth coordinate is useful in a wide range of medical applications covering neuroanatomy,[9,11] cardiac modelling,[12] and cancer treatment planning.[13,14]

*This research has been funded by the Catalan project 2009-TEM-00007, Spanish projects TIN2009-13618, TIN2012-3311, and the European Union FP7 grant agreement no. HEAR-EU 304857

Medical Imaging 2014: Image-Guided Procedures, Robotic Interventions, and Modeling,
edited by Ziv R. Yaniv, David R. Holmes III, Proc. of SPIE Vol. 9036, 903605

Besides, they allow integration of multimodal data across subjects provided that the coordinate system assigns equal values to equivalent anatomical sites.[3,5,15]

Two main methodologies exist for defining volumetric coordinates, volume approximation using basic functions and medial representations. Performance wise, the basic function approach is highly dependent on the type of function such as B-splines or spherical harmonics used to approximate volume geometry. Most methods use spherical harmonics and, thus, restrict to volumes of spherical type, like the brain.[16] Although recent works[17] have applied other basic functions (Hermite polynomials) for generating regular meshes over more complex geometries (like the myocardium), they do not provide, indeed, a parametric mapping. Medial representations[11,18,19] describe anatomical volumes using the perpendicular (radial) direction to the volume medial surface and have been extensively applied to several medical imaging problems.[11,14] Although medial representations suffice to describe volume geometry, they do not provide parametric coordinates. Besides, they are not well suited for description of the medial branches associated to non-convex shapes. A recent work,[20] uses a biharmonic PDE to define a radial coordinate for medial surfaces presenting complex branching topologies. The flexibility of the approach allows the parameterization of anatomies as complex as the myocardium.[15] A main concern is that surface coordinates are given by a discrete triangular mesh of the medial surface and, thus, they might not provide a proper parameterization.

In this work we present a methodology for the definition of coordinate systems of anatomical volumes that contributes to the field in two aspects. First, we present a method that extends current harmonic parameterizations to 3D domains and directly works on the discrete voxel image domain the level curves of the parameterization define a volumetric mesh. Second, our method allows using flexible boundary conditions defined over anatomical structures of complex geometry. Finally our experiments illustrate the potential of our methodology to the parameterization of the liver anatomy for transplant planning.

2. METHODS

2.1 Liver parametrization using heat propagation

Heat equation elliptic PDEs with specific boundary conditions are a powerful tool for defining coordinate systems. Boundary Conditions (BC) take the form of constrained heat values at specified points (Dirichlet BC), or constrained fixed values of a partial derivative at a point (Neumann BC). Dirichlet conditions constrain the values of heat (coordinate values) at some specific anatomical sites, which will be extended by the heat equation to the whole domain. This allows to write generic procedures for the computation of coordinates. Given that different boundary conditions imply completely different coordinate mappings, their setting is crucial for getting a suitable parameterization of the anatomy. Parametric mappings are given by the final steady state solution of heat equation (Laplace equation).

Parametric mappings solve the Laplacian:

$$\Delta u = 0 \qquad u_{|\mathcal{A}} = f \tag{1}$$

for $f = f(x, y, z)$ the coordinate values defined at anatomical specific sites $\mathcal{A}$ that have to be extended to the whole anatomical volume.

By applying the Laplace discrete operator to all image voxels, equation (1) can be written in matrix form as $Au = 0$. The matrix A, also called graph Laplacian, encodes the neighboring relations between voxels.

Boundary conditions are introduced by setting the values of u to specific values at voxels belonging to the anatomical sites $\mathcal{A}$. Those values will act as origin of coordinates and represent the Dirichlet boundary values of our bounday value problem. The solution to the Laplacian with Dirichlet anatomical conditions is obtained by solving the system of equations $Au = b$, with b being a row matrix encoding the boundary values. Abdominal CT scans can be captured at resolutions such as 512x512x300 and the liver is the largest internal organ so it occupies great part of the volume. Using 27-connected neighborhood, the matrix A of a 3D liver can have millions of rows. Although A is sparse by definition, solving the system of equations with standard techniques might be unfeasible. Given that A is symmetric and positive definite we can use Preconditioned Conjugate Gradient

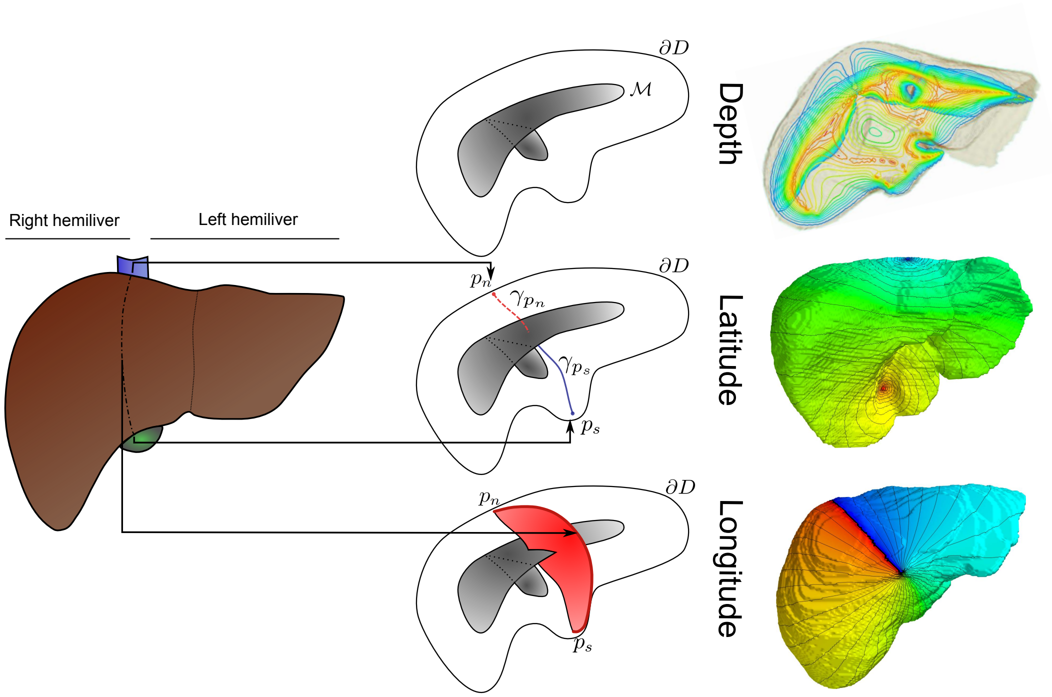

Figure 1. Liver boundary conditions for functional parameterization of the three coordinates.

method using the Incomplete Cholesky Factorization of A as preconditioner.[21] This allows solving the system iteratively in short time and with low memory footprint.

Given that the liver segmentations have no internal holes, the organ is homeomorphic to the sphere. Consequently, we parameterize the volumes using spherical coordinates (latitude, longitude) and adding a third radial or depth coordinate in order to reach the interior points. Boundary conditions are used at specific anatomical landmarks, with ranges latitude $\in [-\pi, \pi]$, longitude $\in [0, 2\pi]$ and radial $\in [0, 1]$.

2.2 Anatomical Boundary Conditions for the Liver

A main requirement for providing a good reference system for the parameterized liver is to select adequate landmarks as origins of coordinates. Although the liver has some anatomical landmarks, it is often much more useful for clinical applications to consider its functional characterization.[1] Boundary conditions will be set according to the functional structure of the liver.

For spherical objects, the radial coordinate can be defined from the heat flowing from the volume center of mass to the external boundary. However, for generic shapes, the center of mass is not a good candidate for radial origin of coordinates. Medial surface is the loci of center of maximal spheres bi-tangent to the surface boundary points of the shape,[18] and by definition,[22] medial surfaces are always located in the center of the object, and they are an excellent candidate from where heat can spread to the surface of the object. The skeleton or medial surface of a shape is not unique, and many different methods generate different medial manifolds, not all of them equally suited to be used in this scenario.[23] We use a method for computation of anatomy-friendly medial surface computation,[24] that generates medial surfaces requiring no pruning and without of extra spurious medial surfaces. These medial surfaces provide good starting point for the radial coordinate.

Let $\mathcal{M}$ be the medial surface and ∂D the anatomical volume boundary. Then, the Dirichlet conditions for defining the radial coordinate are given by:

$$f(x,y,z) = \begin{cases} 1, & \text{for } (x,y,z) \in \mathcal{M} \\ 0, & \text{for } (x,y,z) \in \partial D \end{cases} \qquad (2)$$

Boundary voxels in equation (2) are determined by searching voxels of the object that are n-connected to background voxels.[22,25] The definition of boundary conditions is sketched in the liver scheme of Fig. 1 showing in gray a medial surface of a liver schematic anatomy. An example of radial coordinate (D_ϕ) obtained over a liver volume is shown also, with three axial cuts and a color map encoding radial values.

Latitude D_γ is defined along curves radially traversing the volume and joining two separated points (poles) of the volume boundary, p_n, p_s. These two poles can be placed at different points of the surface boundary, ∂D. The specific selection of pole voxels is application dependent, but in general opposite points in the surface give best results. The gradient of the radial map is used to join the two poles p_n and p_s along two curves, γ_{p_n}, γ_{p_s} that go from each pole to the medial surface. The Dirichlet conditions for defining latitude coordinate are given by:

$$f(x,y,z) = \begin{cases} \pi, \ \text{for } (x,y,z) \in \gamma_{p_n} \\ -\pi, \ \text{for } (x,y,z) \in \gamma_{p_s} \end{cases} \quad (3)$$

In the liver, good candidates for the definition of the poles are the point where the inferior vena cava enters into the liver (north pole) and the gall bladder fossa as south pole. The definition of boundary conditions described by (3) is sketched in the liver scheme of Fig. 1, that shows γ_{p_n} in dashed line and γ_{p_s} in solid one.

Longitude D_ρ spans from an imaginary curve, (a meridian), than runs from pole to pole. The shortest latitude path over ∂D from p_n to p_s may be used. This curve is propagated inwards along the radial gradient until it meets the latitude curves γ_{p_n}, γ_{p_s}, defining a meridian surface, that can be used to define boundary conditions for longitudinal heat propagation.

The meridian surface defines the starting of the longitudinal angular parameter. In order to force periodicity, the end of the longitude is assigned to the the neighbouring voxels lying on the meridian left hand-side. Orientation is defined by the sign of the dot product between the normal vector at the meridian surface and the vector from the current meridian voxel to the next. If we note by MS_+ the meridian surface and by MS_- its left replica, then the Dirichlet conditions for the longitude are given by:

$$f(x,y,z) = \begin{cases} 0, \ \text{for } (x,y,z) \in MS_+ \\ 2\pi, \ \text{for } (x,y,z) \in MS_- \end{cases} \quad (4)$$

In the liver, Cantlie's line is an imaginary line (it is not a physical feature) on the surface of the liver that runs from the inferior vena cava anteriorly to the gall bladder fossa. This line divides the liver into two separated functional hemi-livers. This line will define the starting meridian for the origin of longitudinal coordinate in equation (4). The definition of boundary conditions is sketched in the liver scheme of Fig. 1 that shows the meridian surface in red. The longitude is over a liver colored using latitude values and showing its level curves.

With this set of boundary conditions, parameterized livers map the functional nature of the liver of different patients.

3. RESULTS

In order to illustrate the flexibility of our volumetric coordinates, we have parameterized four liver segmentation masks from the SLiver07 MICCAI challenge.[4] Liver lobe distributions introduce a complex convexity in their shape that is challenging for any medical application. Examples of the parameterized livers can be seen on Fig. 2 a and b. Our radial coordinate agrees with the definition required for medial representations and surface coordinates have been perfectly propagated inside volumes parameterizing all depth levels as depicted on Fig. 2 c.

We also show how the organ-centric coordinate system can be used to quantify the variability of the liver segments. According to Couinaud's rules, the fourth segment of the liver can be found between the planes defined by the middle hepatic vein and the left hepatic vein (Fig. 3a). On the surface of the liver, the segment is limited by the falciform ligament and Cantlie's line. The hemiliver based coordinate system can be used to evaluate the variability in the width of the fourth segment. To that effect we have measured the longitudinal distance from Cantlie's line to the falciform ligament. The four cases depicted in Fig. 3 b to e show the differences of the fourth segment of the liver. The values of the segment size can be seen on Table 1.

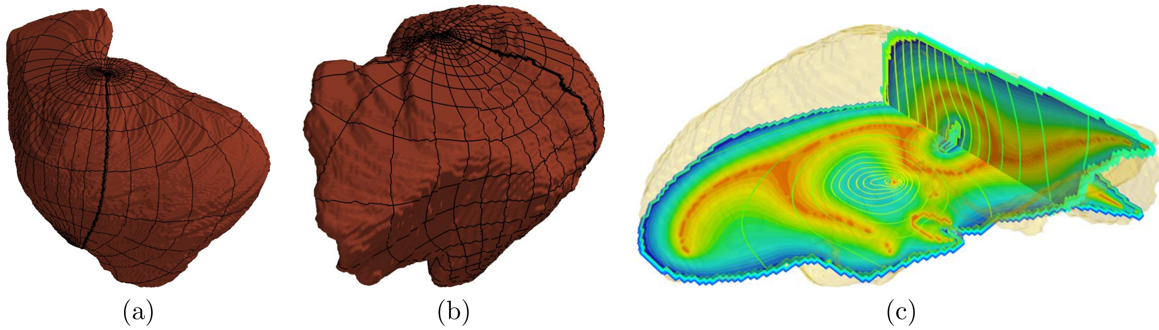

Figure 2. Liver parameterization. Two livers parameterized (a) and (b). Section of the liver where radial, latitude and longitude are visible inside the volume (c).

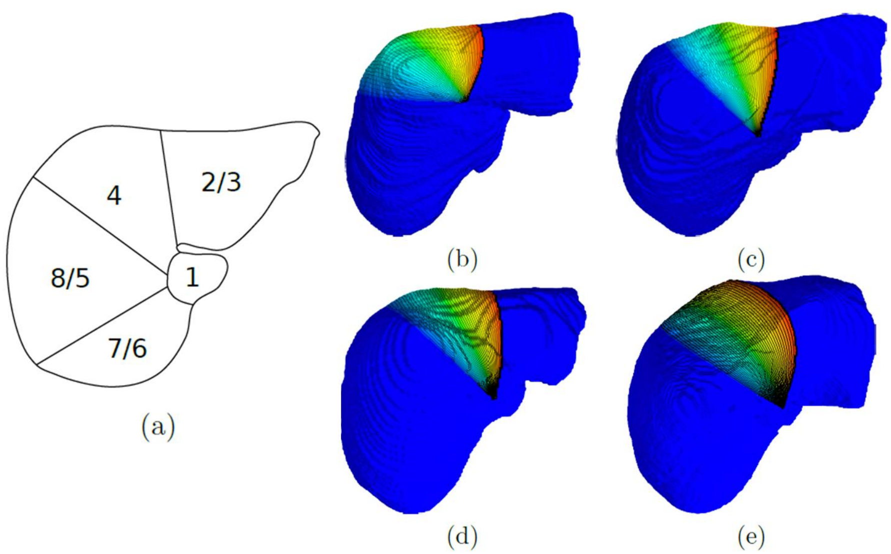

Figure 3. Liver segment size comparison: a) top view segment diagram, b) to e) average distance from Cantlie line to falciform ligament.

Liver	Segment size
Liver 1	2.13 ± 0.27
Liver 2	1.02 ± 0.21
Liver 3	1.01 ± 0.11
Liver 4	1.29 ± 0.10

Table 1. Fourth segment sizes

4. CONCLUSIONS

Most of the existing implementations of harmonic mappings in medical imaging restrict to either anatomical surfaces, or the depth coordinate with boundary conditions is given at sites of limited geometric diversity. In this paper we have presented a flexible method for parameterization and meshing of volumetric anatomical shapes, able to provide a parameterization of the depth coordinate regardless of the volume shape. The possibility of defining flexible organ-centric volumetric meshes providing coordinate systems will allow analysis of intra-organ structures in a domain-specific framework and comparison of their differences. This scheme also enables the comparison between different patients, even in organs with great variability without the need for explicit registration of images. In this way we propose a common parameterization for the liver anatomy based on the functional hemilivers of the organ. Results suggest a promising potential as a tool for patient specific anatomical modeling. Similarly, other parameterizations can be found for different organs as long as a good set of landmarks can be detected as origin of coordinates.

REFERENCES

[1] Couinaud, C., [*Le foie : études anatomiques et chirurgicales*], Masson, Paris (1957).

[2] Fasel, J., Majno, P., and Peitgen, H.-O., "Liver segments: an anatomical rationale for explaining inconsistencies with couinaud's eight-segment concept," *Surgical and Radiologic Anatomy* **32**(8), 761–765 (2010).

[3] Gil, D., Garcia-Barnes, J., and A. Hernandez, A., "Manifold parametrization of the left ventricle for a statistical modelling of its complete anatomy," in [*SPIE*], 304–314 (2010).

[4] Heimann, T., van Ginneken, B., Styner, M. A., Arzhaeva, Y., and Aurich, V., "Comparison and evaluation of methods for liver segmentation from CT datasets," *IEEE Trans. Med. Imag.* **28(8)**, 1251–1265 (2009).

[5] Wang, Y., Gu, X., Hayashi, K. M., Chan, T. F., Thompson, P. M., and Yau, S.-T., "Brain surface parameterization using riemann surface structure," in [*Proce. of the 8th international conference on Medical image computing and computer-assisted intervention*], *MICCAI'05*, 657–665 (2005).

[6] Brechbühler, C., Gerig, G., and Kübler, O., "Parametrization of closed surfaces for 3-d shape description," *Comp. Vis. Imag. Unders* **1** (1995).

[7] Spivak, M., [*A Comprehensive Introduction to Differential Geometry, vol. 1*], Publish or Perish, Inc (1999).

[8] Floater, M. S. and Hormann, K., "Surface parameterization: a tutorial and survey," in [*In Advances in Multiresolution for Geometric Modelling*], 157–186 (2005).

[9] Styner, M., Lieberman, J. A., D., P., and Gerig, G., "Boundary and medial shape analysis of the hippocampus in schizophrenia," *Medical Image Analysis* **8**(3), 197–203 (2004).

[10] Wang, Y., Gu, X., Thompson, P. M., and Yau, S.-T., "3D harmonic mapping and tetrahedral meshing of brain imaging data," *Proceeding of Medical Imaging Computing and Computer Assisted Intervention (MICCAI), St. Malo, France* (2004).

[11] Yushkevich, P., Zhang, H., Simon, T., and Gee, J., "Structure-specific statistical mapping of white matter tracts," *NeuroImage* **41**(2), 448–461 (2008).

[12] Sun, H., Avants, B., Frangi, A., Sukno, F., Gee, J., and Yushkevich, P., "Cardiac medial modeling and time-course heart wall thickness analysis," in [*MICCAI*], *LNCS* **5242**, 766–773 (2008).

[13] Crouch, J., Pizer, S., Chaney, E., and et al, "Automated Finite-Element analysis for deformable registration of prostate images," *TMI* **26(10)**, 1379–1390 (2007).

[14] Stough, J., Broadhurst, R., Pizer, S., and Chaney, E., "Regional appearance in deformable model segmentation," **4584**, 532–543 (2007).

[15] Sun, H., Frangi, A., Wang, H., Sukno, F., Tobon-Gomez, C., and Yushkevich, P. A., "Automatic cardiac mri segmentation using a biventricular deformable medial model," in [*MICCAI 2010*], *LNCS* **6361**, 468–475 (2010).

[16] Kelemen, A., Szekely, G., and Gerig, G., "Elastic model-based segmentation of 3d neuroradiological data sets," *Trans. Med. Imaging* **18**, 828–839 (1999).

[17] Lamata, P., Niederer, S., D.Nordsletten, and et al, "An accurate, fast and robust method to generate patient-specific cubic hermite meshes," *MedIMa* **15**, 801–813 (2011).

[18] Blum, H., [*A transformation for extracting descriptors of shape*], MIT Press (1967).

[19] Pizer, S. and Fletcher, P. e. a., "Deformable M-Reps for 3D medical image segmentation," *Int. J. Comp. Vis.* **55**(2), 85–106 (2003).

[20] Yushkevich, P., "Continuous medial representation of brain structures using the biharmonic PDE," *NeuroImage* **45**(1), 99–110 (2009).

[21] Hestenes, M. R. and Stiefel, E., "Methods of Conjugate Gradients for Solving Linear Systems," *Journal of Research of the National Bureau of Standards* **49**, 409–436 (1952).

[22] Pudney, C., "Distance-ordered homotopic thinning: A skeletonization algorithm for 3D digital images," *Comp. Vis. Imag. Underst.* **72(2)**, 404–13 (1998).

[23] Vera, S., Gil, D., Borràs, A., Linguraru, M. G., and González Ballester, M. A., "Optimal medial surface generation for anatomical volume representations," in [*Abdominal Imaging*], 265–273 (2012).

[24] Vera, S., Gil, D., Borràs, A., Linguraru, M. G., and González Ballester, M. A., "Geometric steerable medial maps," *Machine Visions and Applications* (138).

[25] Malandain, G., Bertrand, G., and Ayache, N., "Topological segmentation of discrete surfaces," *International Journal of Computer Vision* **10**(2), 183–197 (1993).